The CH_2CH_2 + OH Gas Phase Reaction: Formaldehyde and Acetaldehyde Formation Routes

Andrea Lombardi[1,2(✉)], Luca Mancini[1,2], Emília Valença Ferreira de Aragão[1,2], and Lisa Giani[1]

[1] Dipartimento di Chimica, Biologia e Biotecnologie, Università degli Studi di Perugia, Via Elce di Sotto 8, 06123 Perugia, Italy
andrea.lombardi@unipg.it
[2] Master-Tec srl, Via Sicilia 41, 06128 Perugia, Italy

Abstract. In this work we assess the viability of the CH_2CH_2+OH gas phase exothermic route as a mechanism for the formation of formaldehyde and acetaldehyde in the Interstellar Medium. The relevant features of the potential energy surface of the system have been characterized by accurate quantum chemical calculations, identifying the available pathways as a sequence of minimum and transition state structures, with no entry barriers. Preliminary theoretical kinetics calculations have been performed at the low temperature range characteristic of the spatial environments where such neutral-neutral reactions could be of interest.

Keywords: Astrochemistry · Rate constant · Transition state

1 Introduction

Complex Organic Molecules (COMs), defined as organic species made up by more than a few atoms, are routinely detected in the Interstellar Medium (ISM) [1]. The investigation of their reaction mechanisms is a major task of astrochemistry, functional to the explanation of the abundances of the observed molecules and to the identifications of the processes that mostly contribute to their formation. COMs have been discovered under a variable range of extreme conditions typical of different spatial environments, such as cold clouds [2], protostellar envelopes [3] or protoplanetary disks [4], to mention some of them.

The two main types of phenomena allowing for molecules to be generated are (i) grain chemistry, where the surface of dust grains interacts with molecules promoting product formation and (ii) gas-phase reactions upon collisions.

The ISM is characterized by very low temperatures and densities, which essentially reduce the viable gas phase processes to exothermic reactions and to pathways with not too high energy barriers. Even so, there are many fundamental aspects of gas-phase processes that have to be known in detail, among them, the reactive rate coefficients have to be quantified as accurately as possible, for the

© Springer Nature Switzerland AG 2021
O. Gervasi et al. (Eds.): ICCSA 2021, LNCS 12953, pp. 581–593, 2021.
https://doi.org/10.1007/978-3-030-86976-2_39

many possible reactive channels. Moreover, since reactive dynamics and kinetics of the molecular systems are a manifestation of the underlying potential energy surface, an accurate characterization of the electronic states at relevant geometries and energy profiles of the most relevant pathways is a prerequisite to obtain reliable theoretical results. Typical approaches for gas phase reactivity therefore integrate accurate quantum chemical calculations, dynamics simulations and kinetic modelling.

Two important molecules in the ISM, formaldehyde (HCOH) and acetaldehyde (CH_3COH), are the object of this work. Formaldehyde has been detected for the first time in 1969 trough the analysis of ground state rotational transitions against numerous galactic center and extragalactic radio sources, including, as an example, SgrA and SgrB2 [5]. Since that moment the molecule has been detected in a variety of environments, including cold and warm regions. Fomaldehyde, and its deuterated analogue HDCO, has been detected in 1995 toward the Orion Molecular Cloud (OMC-1)[6], while later in the 2000s different regions have been analyzed, including solar-type protostars [7]; Class 0 protostars [8]; cold, dense pre-protostellar cores [9], young stellar objects [10] and Photodissociation regions [11,12]. Most of the models built in order to constrain the abundances of the aforementioned molecule include the formation of formaldehyde through subsequent processes in the surface of the grains, followed by the injection in the gas phase as a consequence of the evaporation of the grain mantles when the temperature reaches 100K. The other target molecule in this work, acetaldehyde is considered as an important precursor for the synthesis of prebiotic species such as carbohydrates and amino acids [13,14]. The first detection of the molecule has been reported in 1973 [15] and later confirmed in 1974 trough the observation of the 211–212 transition in the SgrB2 region [16]. Since that moment, several works revealed the presence of acetaldehyde in different regions including the Orion Molecular Cloud (OMC-1) [17] but also low mass protostars [18,19], cold prestellar cores [20,21] (where the temperature can reach values near 10K) and in the L1157-B1 shock region [22], also related to high-mass protostars [23]. In the last years, the analysis of some data coming from the ALMA telescope allowed the identification of acetaldehyde in Dark clouds [24]. In 2019 new observations have been performed through the vertically resolved disk around a protostar [25], while last year a survey analysis of 31 starless and prestellar cores in the Taurus Molecular Cloud [26] has been reported, together with the detection of acetaldehyde in the shocked material associated with low-mass protostellar outflows [27].

Considering the huge variety of environments in which the CH_3COH molecule has been detected, together with the strong prebiotic potential showed, several formation mechanisms have been proposed in order to understand the possible origin of this species. In particular different gas phase neutral-neutral and ion-neutral reactions have been proposed in the past years starting from dimethyl ether [28], ethyl radical [29] and methanol [30]. A work from Skouteris et al. in 2018 shows the possible formation route of CH_3COH starting from the chemical activation of the ethanol molecule [31], followed by the reaction with atomic

oxygen, while a recent analysis performed by Vazart et al. [32] revised the possible C_2H_5+O(^{3}P) and CH_3OH+CH reactions in order to provide the values of the rate constant in the 7–300 K range of temperature. Other processes can be invoked as possible formation mechanisms of HCOH and CH_3OH in the gas-phase, including the OH+C_2H_4 reaction.

A theoretical analysis of the aforementioned process has been performed by S.J. Klippenstein and collaborators [33] through ab-initio calculations for portions of the PES, together with a kinetic analysis using the two-transition state model, in order to reproduce the experimental data. The calculations showed two possible reaction pathways: (i) the formation of a van der Waals adduct coming from the association of the two species and (ii) an hydrogen abstraction process, leading to the formation of a water molecule. The possible competition between the formation of acetaldehyde and its isomer, vinyl alcohol, is also examined. Similar results have been obtained by R.S. Zhu and coworkers at the PMP2/aug-cc-pVQZ//MP2/cc-pVTZ level of theory coupled with RRKM calculations [34]. A different analysis has been performed by Z.F. Xu et al. and B.J. Ratliff et al. starting from the CH_3CHOH and CH_2CH_2OH radicals respectively [35,36], leading to the formation of C_2H_4 + OH, together with other possible combinations of products, including acetaldehyde and formaldehyde.

In the present work the attention has been focused on the first possible pathway, namely the interaction of the two reactants followed by the formation and evolution of a vdW adduct.

The paper is organized as follows. In Sect. 2 the theoretical and computational methods used for the characterization of the potential energy surface and its relevant stationary points are described. The potential adopted to model the intermolecular interactions characterizing the vdW adduct formation is detailed and a brief description of the kinetic theory is given.

2 Methodology

Here we describe the theoretical approach to the calculation of the stationary points in the reactive pathways of the OH + C_2H_4 system and the rate coefficients for the various elementary steps leading to formaldehyde and acetaldehyde formation. The initial step at the beginning of the two reactive pathways is mediated by the formation of a van der Waals adduct between ethene and the hydroxyl radical, which can subsequently evolve to the hydroxyethyl radical (HER). The adduct formation, a barrierless process, has been modelled by capture theory.

2.1 Electronic Structure Calculations

The OH + C_2H_4 reaction has been analyzed adopting a computational strategy already used in the past for several systems [37–43]. In particular the doublet potential energy surface has been investigated through optimization of the most stable stationary points at the DFT level of theory using the B3LYP functional

[44,45] in conjunction with the correlation consistent valence polarized set aug-cc-pVTZ [46]. The same level of theory has been used to perform harmonic vibrational frequency calculations, in order to determine the nature of each stationary point, classified as minimum if all the frequencies were real and as a first order saddle point (representative of a transition state) if there was a single imaginary frequency. The identified saddle point structures have been assigned using Intrinsic Reaction Coordinate calculations (IRC) [47,48]. Finally refined energy values for each identified stationary point have been obtained using coupled cluster theory, including single and double excitations as well as a perturbative estimate of connected triples CCSD(T) with the same aug-cc-pVTZ basis set [49–51]. All the energies have been corrected by adding the zero point energy, computed using the scaled harmonic vibrational frequencies as obtained at the B3LYP/aug-cc-pVTZ level of theory. All the calculations have been performed using GAUSSIAN09 [52], while the analysis of the vibrational frequencies have been carried out using Avogadro[53].

2.2 Van der Waals Interaction Potential

The initial bimolecular association process is the vdw dimer formation driven by intermolecular forces. A semi-empirical potential function has been adopted to model these interactions and to evaluate the C_6 coefficient used for the kinetic calculations. In details, the overall potential V_{tot} is assumed to be a combination of two terms, as follows:

$$V_{tot} = V_{ILJ} + V_{elect} \tag{1}$$

where V_{elect} is the electrostatic interaction contribution and V_{ILJ} (see next for the subscript acronym) is the contribution due to size repulsion and dispersion attraction, usually named as the vdW term. The electrostatic contribution has been evaluated considering the Coulombic interactions between pairs of charges (see Table 1) obtained from the CCSD(T)/aug-cc-pVTZ calculations for each atom of the two interacting fragments:

$$V_{elect}(r) = \frac{1}{4\pi\varepsilon_0} \sum_{i=1}^{6} \sum_{j=1}^{2} \frac{q_i q_j}{r_{ij}} \tag{2}$$

The non-electrostatic term V_{ILJ} has been evaluated using the so called Improved Lennard-Jones (ILJ) potential function, which provides a better reproduction with respect to the classical Lennard-Jones model over both short- and long-range distances [54]. The ILJ potential, for a pair of interacting centers at a distance r, can be expressed as:

$$V_{ILJ}(r) = \varepsilon \left[\frac{m}{n(r) - m} \left(\frac{r_m}{r} \right)^{n(r)} - \frac{n(r)}{n(r) - m} \left(\frac{r_m}{r} \right)^{m} \right] \tag{3}$$

where ε and r_m are the well depth and position of the potential, respectively, m=6 for neutral-neutral systems and $n(r)$ can be expressed as follows:

Table 1. Mulliken partial charges obtained from the CCSD(T)/aug-cc-pVTZ calculations.

Atom	Mulliken partial charges (CCSD(T))
C	−0.899
H	0.449
O_{rad}	−0.275
H_{rad}	0.275

Table 2. ε and r_m parameters used to obtain the non-electrostatic potential.

Interacting pair	r_m (Å)	ε (meV)
C-O_{rad}	3.62	5.21
H-O_{rad}	3.31	2.61
C-H_{rad}	3.47	2.05
H-H_{rad}	3.07	1.26

$$n(r) = \beta + 4.0\left(\frac{r}{r_m}\right)^2 \tag{4}$$

The β parameter is set equal to 8 in our case. The r_m and ε parameters can be obtained considering the polarizability of the two interacting partners [55]. Their values for this system are listed on Table 2.

2.3 Kinetic Calculations

Kinetic calculations have been performed to derive the rate coefficients for the formation of the two identified products, using a code developed for this purpose in our group. In order to get a rate coefficient for the first step leading to the van der Waals adduct formation, capture theory has been used assuming the following expression for the entrance attractive potential $V(R)$:

$$V(r) = -\frac{C_n}{r^n} \tag{5}$$

where n is equal to 6 in the case of neutral-neutral systems ($n = 4$ for ion-neutral processes), R is the distance between the two particles and C_n is the interaction coefficient between the two species. Subsequently, RRKM theory has been used in order to evaluate all the unimolecular processes, the rate coefficient at a specific energy, $K(E)$, being obtained as follows:

$$K(E) = \frac{N(E)}{h\rho(E)} \tag{6}$$

where $N(E)$ is the sum of states at an energy E, $\rho(E)$ is the density of states, and h is the Planck's constant. A master equation has been solved including all the unimolecular rate coefficients in order to obtain the branching ratios for the formation of the two products.

3 Results

3.1 Electronic Structure Calculations

A schematic version of the Potential Energy Surface (PES) obtained for the OH + C_2H_4 reaction is reported in Fig. 1. For simplicity, only the CCSD(T) energies corrected with the zero-point energy have been reported in the figure. The first step of the reaction appears to be the interaction of the OH radical with the ethylene molecule, leading to the formation of a van der Waals adduct, named INT1, located 7.9 kJ mol^{-1} below the reactant energy asymptote, where the distance between the two interacting fragments is around 2.5 $\AA$. A small barrier of 0.4 kJ mol^{-1} must be overcome in order to form the INT2 intermediate (hydroxyethyl radical), in which is possible to notice the formation of a new C-O chemical bond, with a relative energy of -109.2 kJ mol^{-1}. The related transition state, TS1, clearly shows the rotation of the OH radical and the interaction of the O atom with one of the two carbon atoms of the ethylene molecule. Once INT2 is formed, it can isomerize to INT3 by transferring an hydrogen atom from the oxygen to the carbon. The new intermediate is located 100 kJ mol^{-1} below the reactant energy asymptote, nevertheless a barrier of 131.8 kJ mol^{-1} must be overcome. As a consequence the above mentioned process appears to be endothermic. Tunneling effects can be invoked in order to explain the crossing of the barrier at low temperature conditions when the crossing is classically forbidden. Once INT3 is formed, it can easily undergo dissociation in order to produce the formaldehyde molecule, together with the CH_3 radical. The transition state TS3, which clearly shows the breaking of the C-C bond, is located 25.5 kJ mol^{-1} below the reactant energy asymptote, while the HCOH + CH_3 products show an exothermicity of -53.1 kJ mol^{-1} with respect to the reactants. A different fate can affect INT3: a hydrogen elimination process leading to the formation of acetaldehyde, located 34.3 kJ mol^{-1} below the reactant energy asymptote. The analysis of the vibrational frequencies calculated for the related transition state TS4, which shows a relative energy of -7.5 kJ mol^{-1}, clearly shows the breaking of a C-H bond. In Figs. 2, 3, 4 are reported the geometries of all the stationary points identified along the potential energy surface, together with the reactants and the possible products, obtained at the B3LYP/aug-cc-pVTZ level of theory, while in Table 3 are reported the enthalpy changes and the barrier heights for each step, computed at the CCSD(T)/aug-cc-pVTZ level.

3.2 Van der Waals Interaction Potential

The overall interaction potential $V(r)$, in kJ mol^{-1}, as a function of the distance between the two reactants is reported in Fig. 5. The plot clearly shows a minimum in the potential at a distance between the H atom of the OH radical and the center of mass of the ethylene molecule of 2.6 $\AA$, which appears to be in agreement with the data coming from electronic structure calculations, where the distance between the two interacting atoms of the fragments is $d_{C-H} = 2.517$ $\AA$, while the energy coming from the semi-empirical potential appears to be 6.95 kJ mol^{-1} lower than the

Table 3. Enthalpy changes and barrier heights (kJ mol^{-1}, 0 K) computed at the CCSD(T)/aug-cc-pVTZ level of theory for the system OH + C_2H_4.

Reaction path	ΔH_0^0 kJ mol^{-1}	Barrier Heights kJ mol^{-1}
OH + C_2H_4 → INT1	−7.9	
INT1 → INT2	−101.3	0.4
INT2 → INT3	9.2	131.8
INT3 → CH_3 + HCOH	46.9	74.5
INT3 → H + $HCOCH_3$	65.7	92.6

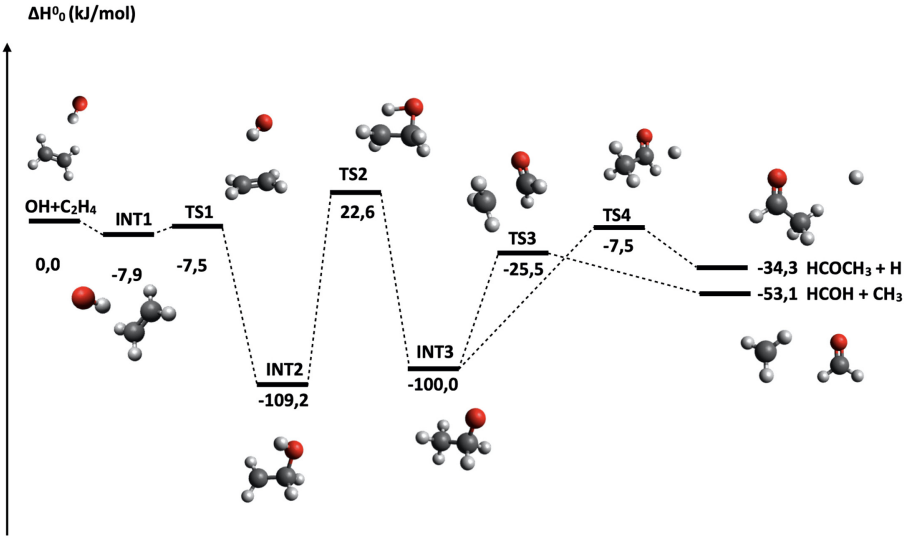

Fig. 1. Schematic version of the Potential Energy Surface including the energies obtained at the CCSD(T)/aug-cc-pVTZ level of theory.

CCSD(T)/aug-cc-pVTZ energy. The data related to the long-range interaction, particularly the range of distances from 2 $\AA$ to 5 $\AA$, have been used in a fitting procedure in order to obtain the value of the C_6 coefficient, to be included in the kinetics calculations for the estimation of the branching ratios.

3.3 Kinetic Calculations

According to our analysis, the first step of the reaction is the interaction of the two reactants and the barrierless formation of a van der Waals adduct. A small barrier leads to the formation of an intermediate with a new C-O bond. Alternatively the adduct has the option of undergoing back dissociation to the reactants. The RRKM analysis has been carried out on the PES described in the previous sections. In the case of back dissociation, the rate is proportional

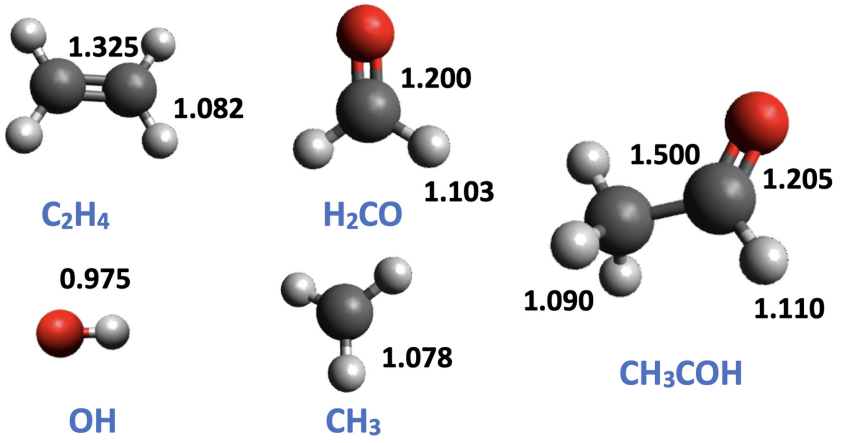

Fig. 2. Main distances (in $\AA$) of the reactants and products for the OH+C_2H_4 reaction obtained at the B3LYP/aug-cc-pVTZ level of theory.

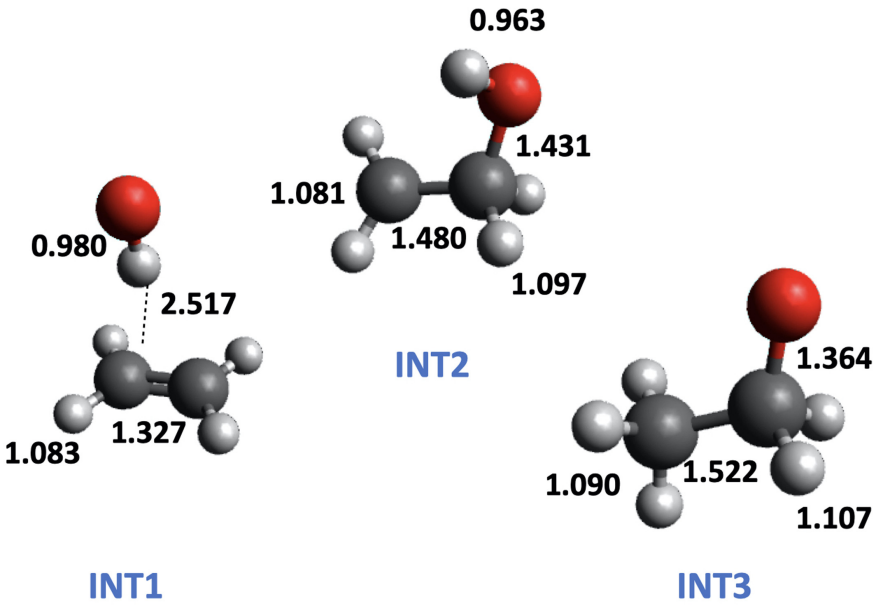

Fig. 3. Main distances (in $\AA$) of the intermediates for the OH+C_2H_4 reaction obtained at the B3LYP/aug-cc-pVTZ level of theory.

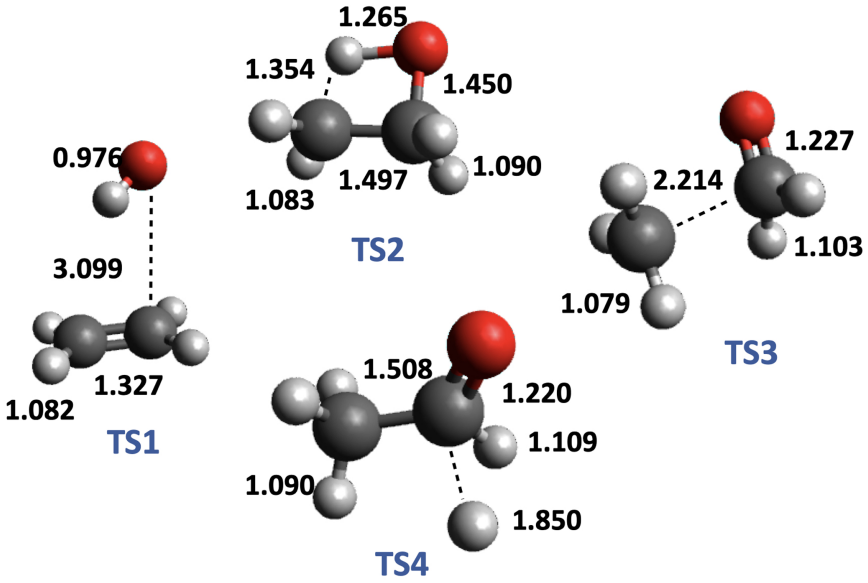

Fig. 4. Main distances (in $\AA$) of the saddle points for the OH+C_2H_4 reaction obtained at the B3LYP/aug-cc-pVTZ level of theory.

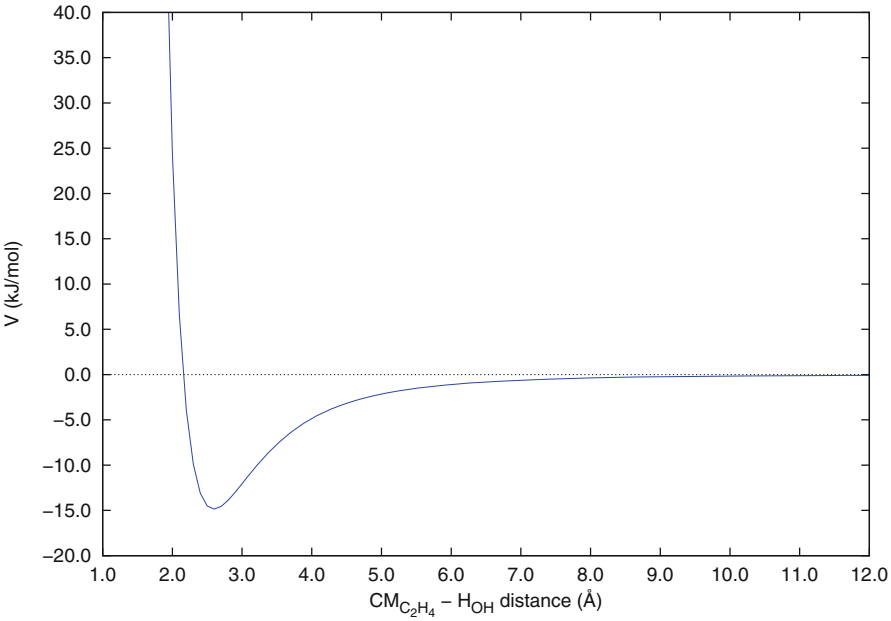

Fig. 5. Interaction potential [kJ mol^{-1}] as a function of the distance between the two reactants [$\AA$].

to the density of states of the reactants. The obtained branching ratios for the formation of the two products are reported in Table 4. As it can be noticed, in the range of temperatures between 1 and 300 K the % of formation of the two products is almost negligible, while the only possible process appears to be the back dissociation. This is due to the presence of TS2, located 22.6 kJ mol^{-1} above the energy of the reactants, which makes the reaction inefficient under the conditions of the Interstellar Medium. Only a small fraction of the reactive flux can lead to the formation of formaldehyde at 10K. This process can be explained considering the possibility of tunneling at low temperatures, allowing the system to reach the configuration of INT3. Once INT3 is formed, it can dissociate to form both acetaldehyde and formaldehyde. The breaking of the C-C bond appears to be favourable, due to the lower barrier heights. As a consequence the formation of formaldehyde is preferred with respect to acetaldehyde.

Table 4. Branching ratios (%) obtained for the formation of the two products identified in the PES

Temperature (K)	HCOH + CH_3 (%)	CH_3CHO + H (%)
10	3.255	0.0196
50	0.0377	0.0002
100	0.0056	0.00004
200	0.0012	0.00001
300	0.0008	0.00001

4 Conclusions and Future Works

In the present work we analyzed the reaction between the OH radical and the ethylene molecule. Theoretical quantum chemical calculations allowed us to describe the formation of two different products: formaldehyde and acetaldehyde. An initial barrierless association process has been identified, nevertheless an endothermic transition state has been found to be related to a rearrangement process, fundamental for the formation of the title products. As a consequence the investigated reaction pathways can not be considered the main formation mechanisms of the two aforementioned species under the harsh conditions of the Interstellar Medium, given the inefficiency of the processes. A more detailed analysis will be performed in the future in order to identify other possible reaction pathways, including the H-abstraction channel.

Acknowledgments. The work presented in this paper has received funding from the European Union's Horizon 2020 research and innovation programme under the Marie Skłodowska-Curie grant agreement No 811312 for the project "Astro-Chemical Origins" (ACO). EVFA thanks the DICA (Dipartimento di eccellenza) of University of Perugia for allocated computing time. AL and NFL thank the Dipartimento di Chimica, Biologia e Biotecnologie dell'Università di Perugia (FRB, Fondo per la Ricerca di Base

2019 and 2020) and the Italian MIUR and the University of Perugia for the financial support of the AMIS project through the program "Dipartimenti di Eccellenza". AL acknowledges the Italian Space Agency (ASI) Life in Space project (ASI N. 2019-3-U.0). AL and NFL thank the OU Supercomputing Center for Education & Research (OSCER) at the University of Oklahoma, for allocated computing time.

References

1. Caselli, P., Ceccarelli, C.: Our astrochemical heritage. Astron. Astrophys. Rev. **20**, 56 (2012)
2. Aikawa, Y., et al.: AKARI observations of ice absorption bands towards edge-on young stellar objects. A&A **538**, A57 (2012)
3. Aikawa, Y., Nomura, H.: Physical and chemical structure of protoplanetary disks with grain growth. Astrophys. J. **642**(2), 1152–1162 (2006)
4. Aikawa, Y., Umebayashi, T., Nakano, T., Miyama, S.M.: Evolution of molecular abundances in protoplanetary disks with accretion flow. Astrophys. J. **519**(2), 705–725 (1999)
5. Snyder, L.E., Buhl, D., Zuckerman, B., Palmer, P.: Microwave detection of interstellar formaldehyde. Phys. Rev. Lett. **22**, 679 (1969)
6. Sutton, E., Peng, R., Danchi, W., Jaminet, P., Sandell, G., Russell, A.: The distribution of molecules in the core of OMC-1. Astrophys. J. Suppl. Ser. **97**, 455–496 (1995)
7. Ceccarelli, C., Loinard, L., Castets, A., Tielens, A., Caux, E.: The hot core of the solar-type protostar IRAS 16293-2422: H_2CO emission. Astron. Astrophys. **357**, L9–L12 (2000)
8. Maret, S., et al.: The H2CO abundance in the inner warm regions of low mass protostellar envelopes. Astron. Astrophys. **416**, 577–594 (2004)
9. Young, K.E., Lee, J.E., Evans, N.J., II., Goldsmith, P.F., Doty, S.D.: Probing preprotostellar cores with formaldehyde. Astrophys. J. **614**, 252 (2004)
10. Araya, E., Hofner, P., Goss, W., Linz, H., Kurtz, S., Olmi, L.: A search for formaldehyde 6 cm emission toward young stellar objects. II. H2CO and H110α observations. Astrophys. J. Suppl. Ser. **170**, 152 (2007)
11. Guzmán, V., et al.: The IRAM-30 m line survey of the horsehead PDR-IV. comparative chemistry of H2CO and CH3OH. Astron. Astrophys. **560**, A73 (2013)
12. Guzmán, V., Pety, J., Goicoechea, J., Gerin, M., Roueff, E.: H2CO in the horsehead PDR: photo-desorption of dust grain ice mantles. Astron. Astrophys. **534**, A49 (2011)
13. Pizzarello, S., Weber, A.L.: Prebiotic amino acids as asymmetric catalysts. Science **303**, 1151 (2004)
14. Córdova, A., Ibrahem, I., Casas, J., Sundén, H., Engqvist, M., Reyes, E.: Amino acid catalyzed neogenesis of carbohydrates: a plausible ancient transformation. Chem.-A Eur. J. **11**, 4772–4784 (2005)
15. Gordon, M., Snyder, L., Chaisson, E.J.: Molecules in the galactic environment. Phys. Today **28**, 74 (1975)
16. Fourikis, N., Sinclair, M., Robinson, B., Godfrey, P., Brown, R.: Microwave emission of the 211–212 rotational transition in interstellar acetaldehyde. Aust. J. Phys. **27**, 425–430 (1974)
17. Blake, G.A., Sutton, E., Masson, C., Phillips, T.: Molecular abundances in OMC-1: the chemical composition of interstellar molecular clouds and the influence of massive star formation. Astrophys. J. **315**, 621–645 (1987)

18. Cazaux, S., et al.: The hot core around the low-mass protostar IRAS 16293–2422: scoundrels rule! Astrophys. J. Lett. **593**, L51 (2003)
19. Bianchi, E., et al.: The census of interstellar complex organic molecules in the class i hot corino of SVS13-a. Mon. Not. R. Astron. Soc. **483**, 1850–1861 (2019)
20. Bacmann, A., Taquet, V., Faure, A., Kahane, C., Ceccarelli, C.: Detection of complex organic molecules in a prestellar core: a new challenge for astrochemical models. Astron. Astrophys. **541**, L12 (2012)
21. Vastel, C., Ceccarelli, C., Lefloch, B., Bachiller, R.: The origin of complex organic molecules in prestellar cores. Astrophys. J. Lett. **795**, L2 (2014)
22. Lefloch, B., et al.: L1157-B1, a factory of complex organic molecules in a solar-type star-forming region. Mon. Notices Royal Astron. Soc.: Lett. **469**, L73–L77 (2017)
23. Csengeri, T., Belloche, A., Bontemps, S., Wyrowski, F., Menten, K., Bouscasse, L.: Search for high-mass protostars with alma revealed up to kilo-parsec scales (sparks)-II. Complex organic molecules and heavy water in shocks around a young high-mass protostar. Astron. Astrophys. **632**, A57 (2019)
24. Sakai, T., et al.: *Alma* observations of the IRDC clump G34.43+00.24 MM3: complex organic and deuterated molecules. Astrophys. J. **857**, 35 (2018)
25. Lee, C.F., Codella, C., Li, Z.Y., Liu, S.Y.: First abundance measurement of organic molecules in the atmosphere of HH 212 protostellar disk. Astrophys. J. **867**, 63 (2019)
26. Scibelli, S., Shirley, Y.: Prevalence of complex organic molecules in starless and prestellar cores within the taurus molecular cloud. Astrophys. J. **891**, 73 (2020)
27. De Simone, M., et al.: Seeds of life in space (SOLIS)-X. interstellar complex organic molecules in the NGC 1333 IRAS 4A outflows. Astron. Astrophysi. **640**, A75 (2020)
28. Wakelam, V., et al.: A kinetic database for astrochemistry (KIDA). Astrophys. J. Suppl. Ser. **199**, 21 (2012)
29. McElroy, D., Walsh, C., Markwick, A., Cordiner, M., Smith, K., Millar, T.: The UMIST database for astrochemistry 2012. Astron. Astrophys. **550**, A36 (2013)
30. Vasyunin, A.I., Caselli, P., Dulieu, F., Jiménez-Serra, I.: Formation of complex molecules in prestellar cores: a multilayer approach. Astrophys. J. **842**, 33 (2017)
31. Skouteris, D., et al.: The genealogical tree of ethanol: gas-phase formation of glycolaldehyde, acetic acid, and formic acid. Astrophys. J. **854**, 135 (2018)
32. Vazart, F., Ceccarelli, C., Balucani, N., Bianchi, E., Skouteris, D.: Gas-phase formation of acetaldehyde: review and new theoretical computations. Mon. Not. R. Astron. Soc. **499**, 5547–5561 (2020)
33. Senosiain, J.P., Klippenstein, S.J., Miller, J.A.: Reaction of ethylene with hydroxyl radicals: a theoretical study. J. Phys. Chem. A **110**, 6960–6970 (2006)
34. Zhu, R., Park, J., Lin, M.C.: Ab initio kinetic study on the low-energy paths of the HO+C2H4 reaction. Chem. Phys. Lett. **408**, 25–30 (2005)
35. Xu, Z.F., Xu, K., Lin, M.C.: Ab initio kinetics for decomposition/isomerization reactions of C2H5O radicals. ChemPhysChem **10**, 972–982 (2009)
36. Ratliff, B.J., Alligood, B.W., Butler, L.J., Lee, S.H., Lin, J.J.M.: Product branching from the CH2CH2OH radical intermediate of the OH+ ethene reaction. J. Phys. Chem. A **115**, 9097–9110 (2011)
37. de Petris, G., Cartoni, A., Rosi, M., Barone, V., Puzzarini, C., Troiani, A.: The proton affinity and gas-phase basicity of sulfur dioxide. ChemPhysChem **12**(1), 112–115 (2011)
38. Leonori, F., et al.: Observation of organosulfur products (thiovinoxy, thioketene and thioformyl) in crossed-beam experiments and low temperature rate coefficients for the reaction S (1 D)+ C 2 H 4. Phys. Chem. Chem. Phys. **11**(23), 4701–4706 (2009)

39. de Petris, G., Rosi, M., Troiani, A.: SSOH and HSSO radicals: an experimental and theoretical study of [s2oh] 0/+/-species. J. Phys. Chem. A **111**(28), 6526–6533 (2007)
40. Rosi, M., Falcinelli, S., Balucani, N., Casavecchia, P., Skouteris, D.: A theoretical study of formation routes and dimerization of methanimine and implications for the aerosols formation in the upper atmosphere of titan. In: Murgante, B., et al. (eds.) ICCSA 2013. LNCS, vol. 7971, pp. 47–56. Springer, Heidelberg (2013). https://doi.org/10.1007/978-3-642-39637-3_4
41. Skouteris, D., et al.: Interstellar dimethyl ether gas-phase formation: a quantum chemistry and kinetics study. Mon. Not. R. Astron. Soc. **482**(3), 3567–3575 (2019)
42. Sleiman, C., El Dib, G., Rosi, M., Skouteris, D., Balucani, N., Canosa, A.: Low temperature kinetics and theoretical studies of the reaction CN+ CH 3 NH 2: a potential source of cyanamide and methyl cyanamide in the interstellar medium. Phys. Chem. Chem. Phys. **20**(8), 5478–5489 (2018)
43. Berteloite, C., et al.: Low temperature kinetics, crossed beam dynamics and theoretical studies of the reaction s (1 D)+ CH 4 and low temperature kinetics of S (1 D)+ C 2 H 2. Phys. Chem. Chem. Phys. **13**(18), 8485–8501 (2011)
44. Becke, A.D.: Density functional thermochemistry. III. The role of exact exchange. J. Chem. Phys. **98**(7), 5648–5652 (1993)
45. Stephens, P.J., Devlin, F.J., Chabalowski, C.F., Frisch, M.J.: *Ab Initio* calculation of vibrational absorption and circular dichroism spectra using density functional force fields. J. Phys. Chem. **98**(45), 11623–11627 (1994)
46. Dunning Jr, T.H.: Gaussian basis sets for use in correlated molecular calculations. I. the atoms boron through neon and hydrogen. J. Chem. Phys. **90**(2), 1007–1023 (1989)
47. Gonzalez, C., Schlegel, H.B.: An improved algorithm for reaction path following. J. Chem. Phys. **90**(4), 2154–2161 (1989)
48. Gonzalez, C., Schlegel, H.B.: Reaction path following in mass-weighted internal coordinates. J. Phys. Chem. **94**(14), 5523–5527 (1990)
49. Bartlett, R.J.: Many-body perturbation theory and coupled cluster theory for electron correlation in molecules. Annu. Rev. Phys. Chem. **32**(1), 359–401 (1981)
50. Raghavachari, K., Trucks, G.W., Pople, J.A., Head-Gordon, M.: A fifth-order perturbation comparison of electron correlation theories. Chem. Phys. Lett. **157**(6), 479–483 (1989)
51. Olsen, J., Jørgensen, P., Koch, H., Balkova, A., Bartlett, R.J.: Full configuration-interaction and state of the art correlation calculations on water in a valence double-zeta basis with polarization functions. J. Chem. Phys. **104**(20), 8007–8015 (1996)
52. Frisch, M., et al.: Gaussian 09, Revision A. 02, 2009, Gaussian. Inc., Wallingford CT (2009)
53. Hanwell, M.D., Curtis, D.E., Lonie, D.C., Vandermeersch, T., Zurek, E., Hutchison, G.R.: Avogadro: an advanced semantic chemical editor, visualization, and analysis platform. J. Cheminform. **4**(1), 1–17 (2012)
54. Pirani, F., Brizi, S., Roncaratti, L.F., Casavecchia, P., Cappelletti, D., Vecchiocattivi, F.: Beyond the lennard-jones model: a simple and accurate potential function probed by high resolution scattering data useful for molecular dynamics simulations. Phys. Chem. Chem. Phys. **10**(36), 5489–5503 (2008)
55. Cambi, R., Cappelletti, D., Liuti, G., Pirani, F.: Generalized correlations in terms of polarizability for van der Waals interaction potential parameter calculations. J. Chem. Phys. **95**(3), 1852–1861 (1991)